Energy Conversion and Management 326 (2025) 119477

Contents lists available at ScienceDirect

Energy Conversion and Management

journal homepage: www.elsevier.com/locate/enconman

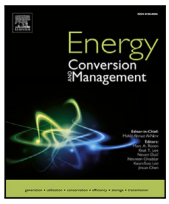

Research paper

Component sizing and dynamic simulation of a low-emission power plant for cruise ships with solid oxide fuel cells

B.N. van Veldhuizen [a,*], L. van Biert [a], C. Ünlübayir [b], K. Visser [a], J.J. Hopman [a], P.V. Aravind [c]

[a] Section Ship Design, Production and Operations, Delft University of Technology, Mekelweg 5, 2628 CD Delft, The Netherlands
[b] Institute for Power Electronics and Electrical Drives (ISEA), RWTH Aachen University, Campus-Boulevard 89, 52074 Aachen, Germany
[c] Energy Conversion, Energy and Sustainability Research Institute, University of Groningen, Nijenborgh 6, 9747 AG Groningen, The Netherlands

ARTICLE INFO

Keywords:
Solid oxide fuel cell
Ship power plant
Emission reduction
Time-domain simulation
Energy management strategy

ABSTRACT

Solid oxide fuel cell systems are considered for the power plant of ships, because of their high efficiency, low pollutant emissions, and fuel flexibility. This research compares the volume, mass, fuel consumption, and emissions of different hybrid power plants for cruise ships using solid oxide fuel cells, fuelled with marine gas oil and liquefied natural gas. A component sizing model allocates the installed power over the selected power plant components and determines their size and weight. The components and energy management strategy are simulated with a cruise ship for five years of operation. A simple method is implemented to estimate the degradation and its effect on component operation. The combined component sizing and time-domain model highlights the importance of dynamic simulation for battery sizing. The results show that using solid oxide fuel cells for the auxiliary consumers can reduce greenhouse gas emissions by 21% and pollutants by 38% to 46% with only 17.5% installed power, which has limited consequences for the cost and size of the power plant. With 31% installed power, the ship can operate in low-emission zones while reducing greenhouse gas emissions by 33% and pollutants by 60% to 70%. Performing all cruise operations requires 51% installed fuel cell power and reduces greenhouse gas emissions by 49% and pollutants by 94% to 96%. In conclusion, the study affirms that solid oxide fuel cell systems, with proper sizing and energy management, can be used to reduce shipping emissions and reach IMO's 30% GHG emission reduction target for 2030.

1. Introduction

In 2022, international shipping accounted for approximately 2% of global CO_2 emissions [1]. Liquefied Natural Gas (LNG) has been implemented as bunker fuel to reduce emissions in the short term and constitutes 15% of newly ordered vessels [2]. However, recent emission measurements on LNG-fuelled vessels report a higher than anticipated methane slip, especially for 4-stroke engines. Comer et al. [3] recommends that a default methane slip of 6% should be considered for policymaking. For the longer term, the marine industry is considering fuels that can be produced renewably, such as hydrogen, ammonia and methanol to reduce carbon emissions over their life cycle [4]. Besides greenhouse gases (GHG), the combustion of marine fuels emits large amounts of nitrogen oxides (NO_X), carbon monoxide (CO), sulphur oxide (SO_X) and particulate matter (PM). The International Marine Organisation (IMO) forces ship operators to reduce greenhouse gas emissions with the Energy Efficiency Existing Ship Index (EEXI) and the Carbon Intensity Indicator (CII) [5]. These regulations contribute to the IMO targets of 30% GHG emission reduction by 2030 and 80% by 2040 [6]. Moreover, strict limits are set to emissions of nitrogen oxides, carbon monoxides and sulphur oxides, especially in dedicated emission control areas [7].

Solid oxide fuel cell (SOFC) systems are a potential solution to reduce greenhouse and pollutant emissions [8]. The high electrical efficiency of 50% to 60% results in fuel savings and thus in a reduction of carbon emissions, compared to marine combustion engines. Moreover, unused fuel is burned in a catalytic after-burner to maintain the temperature of the stack, removing any methane slip, which Baldi et al. [9] identified as the strongest driver of GHG emission reduction. Since power is generated by electrochemical conversion instead of combustion, SOFCs emit almost no NO_X and CO emissions. In the NAUTILUS project, PM emissions are even reported to be lower than ambient conditions, improving the air quality of the direct environment.

SOFC systems offer additional benefits for maritime vessels. SOFCs can operate on different fuels. Natural gas, hydrogen and ammonia can

* Corresponding author.
E-mail address: b.n.vanveldhuizen@tudelft.nl (B.N. van Veldhuizen).

https://doi.org/10.1016/j.enconman.2024.119477
Received 31 August 2024; Received in revised form 19 November 2024; Accepted 31 December 2024
Available online 17 January 2025

Nomenclature

AC	alternating current
AUX	auxiliaries
BAT	battery
BOIL	boiler
BOP	balance of plant
DC	direct current
DFG	dual-fuel generator
DG	diesel generator
DOD	depth of discharge
ECA	emission control area
GG	gas generator
GHG	greenhouse gases
ICE	internal combustion engine
IMO	International Maritime Organisation
LHV	lower heating value
LNG	liquefied natural gas
MAN	manoeuvring
MGO	marine gas oil
NO_X	nitrous oxides
PM	particulate matter
SO_X	sulphurous oxides
SOC	state of charge
SOFC	solid oxide fuel cell
SOH	state of health
TTW	tank-to-wake
WHR	waste heat recovery
WTT	well-to-tank

be directly fed to SOFCs [10], while other carbon fuels can be used after reforming. Moreover, SOFC systems are silent, do not produce vibrations, and offer high redundancy [11]. Nevertheless, SOFCs are not widely applied in ships yet. Currently, their capital costs are much higher and the volumetric and gravimetric power density is much lower than for internal combustion engines [12]. Moreover, the long start-up and shut-down time introduce challenges in operating these systems, especially for ships with dynamic operating profiles. For these reasons, most studies only include SOFCs as an auxiliary power unit resulting in hybrid SOFC-engine-battery power plants [9]. Nevertheless, researchers and industry acknowledge the potential of SOFC systems to reduce ship emissions, especially for ocean-going vessels, for which hydrogen- or battery-based propulsion cannot fulfil the range demands due to low energy density [9].

SOFC systems are often praised for their high combined heat and power efficiency, ranging up to 90% [13], from which applications with a significant thermal load can benefit, such as cruise ships [14]. Although SOFCs operate at temperatures around 700 °C, high-temperature heat recovery is limited because much heat is used internally to bring the air and fuel to the operating temperature of the fuel cells [15]. Baldi et al. [9] points out that few studies also include the thermal balance between the SOFCs, engines and boilers, and the heat users. Rivarolo et al. [16] studied the thermal integration of SOFCs for a cruise ship and concluded that SOFC systems cannot fulfil all the heat demands of the ship. In this study, the thermal balance is also tackled. Boilers are employed and sized accordingly to supply the heat deficit of the other power plant components. Thus, components with low heat recovery capacity directly increase fuel consumption.

SOFC systems operate on high electrical efficiency, with peak efficiency at part-load. This fundamentally differs from internal combustion engines (ICEs) which often operate most efficiently at their rated power. High part-load efficiency can be exploited for ships, because they do not usually sail at their maximum speed. Nevertheless, most integration studies operate SOFCs constantly at full power because of their slow modulation [9], but this results in suboptimal fuel conversion. Haseltalab et al. [17] simulated a hybrid power plant of a dredger with SOFCs, ICE-generator sets (gensets) and batteries. They used load curves to estimate the fuel consumption but neglected the load-dependency of emissions. For combustion, NO_X and CO emission factors are higher at part-load conditions [18]. Furthermore, methane slip up to 12% was measured at part-load conditions [3]. Load-dependent emissions of commercial SOFC systems are not widely published, but a recent measurement campaign reports emission factors for different load cases [19]. Although often neglected in earlier power plant simulations, this study includes the efficiency as well as emissions of power plant components under different load conditions.

SOFC systems typically respond slower to load transients than combustion engines [20]. Rapidly increasing the current introduces hot spots in the stack, which can cause permanent damage [21]. Moreover, the SOFC system and its hot balance of plant components exhibit notable thermal inertia in response to alterations in operational temperature [22]. For this reason, SOFCs are often coupled with batteries for ramp support, load smoothing and/or peak shaving [9]. Simple methods assume a fixed ratio between SOFC and battery capacity [23] and Haseltalab et al. [17] sized the battery capacity as a function of the transient capabilities of the installed SOFCs and engines. However, the required power and energy capacity of the battery is highly dependent on the function it should fulfil and the load profile. In this study, the operational profile of a specific ship application is used to validate the estimated battery capacity and adapted if necessary.

Cell degradation decreases the performance of SOFC systems over their lifetime. Consequently, the stacks need replacement every 40k [9] to 50k [24] running hours. This is often included in techno-economic assessments [25] but not usually considered for power plant simulations. The degradation of SOFCs is a combination of different mechanisms, and models are complex combinations of electrochemistry mechanics and mass transport [26]. Comprehensive degradation simulation includes physics-based models for nickel coarsening and oxidation, conductivity changes of electrolyte and electrodes, sulphur poisoning, and delamination [27]. Such models are too computationally heavy to include in a long-term power plant analysis. Moreover, empirical data for degradation in part-load or even transient operation is not available in the literature. Nevertheless, degradation influences the operational conditions of the SOFC system; an effective degradation model is needed for dynamic simulations. For consistency, performance degradation of engines and batteries should also be considered, especially because reducing the transient load of one component will increase the cycling of the other power-producing components of a hybrid power plant. Cichowicz et al. [28] indicate that the fuel consumption of engines increases with 4.5% over 100k running hours due to wear and fouling of its components. The degradation of lithium-ion batteries varies widely for different battery chemistries but is usually modelled as a combination of calendar ageing and cycling loading [29]. This study includes methods to incorporate component degradation effectively in long-term power plant simulation.

A suitable control strategy is essential to operate a hybrid power plant efficiently. Rule-based control strategies can be employed to distribute the load over the components considering operating points with low fuel consumption or low emissions [30]. More complex strategies, such as model predictive control can be used to further improve energy efficiency, however, for such strategies, a predictable or repetitive load profile is often required [31]. Furthermore, health-aware energy management strategies for hybrid power generation adapt the load distribution based on the associated degradation effects [32]. Energy management strategies that use batteries for load support typically base the required load of the SOFCs on the state of charge (SOC) of the battery [33]. This enables sufficient charge and discharge capacity

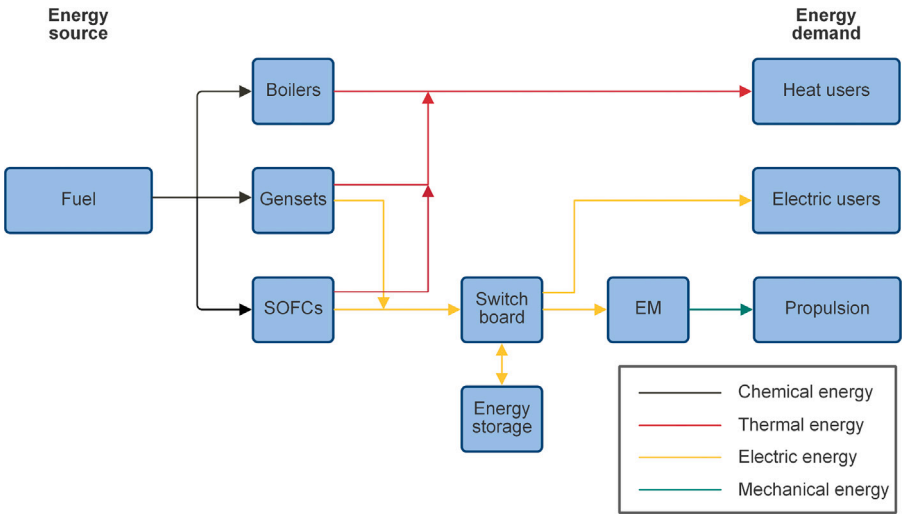

Fig. 1. General system layout of onboard components.

to compensate the SOFC at any moment. Although energy management for hybrid power generation on ships is studied extensively, few manuscripts consider power plants with SOFCs, gensets and batteries [17]. This study implements an energy management strategy considering efficient operation and lifetime preservation of the different power plant components.

To the authors' knowledge, the size, mass, fuel consumption, GHG emissions, and pollutant emissions of hybrid SOFC plants have not been integrally evaluated for cruise ships. Although Li et al. [23] extensively studied the performance of a SOFC, engine, and battery power plant for cargo ships, degradation effects and emissions were not considered in the evaluation, which are included in this study. A dynamic simulation model combining electrical and heat demand, and allocating power among power plant components considering part-load operation, is required for a detailed estimation. Additionally, a low-computational method is necessary to account for the effects of degradation on the operation of SOFC systems.

This research aims to compare the volume, mass, fuel consumption and emissions of different hybrid SOFC power plants for cruise ships. A dynamic power plant model is developed to simulate the control and operation of the needed components. The model can be used to find the right hybridisation strategy for the dedicated ship application. The main contributions of this paper can be summarised as follows:

- The development of a dynamic power plant simulation model that includes component sizing, part-load behaviour, and emissions for the main components that generate electricity or heat.
- Component degradation and its effect on operation is included, which is often neglected in power plant analyses.
- An extensive comparison of power plant size and weight, fuel consumption, and emissions for different hybrid design scenarios.
- Validation and eventually adaption of the required battery and boiler capacity, preventing over- or under-sizing.
- A simple but robust control strategy for the operation of SOFC systems paired with batteries and engines.

2. Methods

The component sizing and power plant simulation is based on the general layout described in Fig. 1. Electrical power is supplied by natural gas-fuelled SOFCs and ICE generator sets, running on marine gas oil (MGO) or natural gas. Batteries are used to support the load-following capability. A waste heat recovery system retrieves heat if needed from the gensets and the SOFCs, which the boilers can complement. An energy management system ensures all electrical and heat demand is met. This section describes how this system is sized and how the different components are modelled in the dynamic simulation model. This model is used to compare different design scenarios quantitatively on the main performance indicators of power plants: volume, weight, fuel consumption, and emissions [22]. CO_2 and CH_4 are included as GHG emissions and NO_X, SO_X, PM, and CO as pollutant emissions, taking into account well-to-tank (WTT) and tank-to-wake (TTW) processes.

2.1. Design scenarios

Multiple reference design scenarios (1-3) and SOFC design scenarios (A-D) are defined in correspondence with two cruise shipyards. Although this does not ensure an optimally sized power plant, these are plausible scenarios from a functional perspective.

- Scenario 1 represents a conventional ship fully powered with MGO-fuelled diesel generators (DGs).
- Scenario 2 has a state-of-the-art power plant with dual fuel gensets (DFG) on MGO and LNG.
- In scenario 3, the use of MGO is eliminated and the ship is fully powered by gas generators (GG).
- Scenario A - SOFC AUX uses SOFCs solely for hotel and auxiliary power demands. The auxiliary (AUX) load is more continuous, even when the ship is berthed. This prevents the need to turn off the SOFCs and limits the required battery capacity.
- Design scenario B - SOFC MAN incorporates sufficient installed power for berthing and manoeuvring (MAN) operations, enabling navigation in ports or fjords with stringent pollutant emission regulations.
- In design scenario C - SOFC CRUISE, sufficient SOFC power is installed to accommodate power requirement for the propulsion and auxiliaries for regular cruise operations, while additional GGs are installed for high-speed cruising and to meet the overall power demand.
- Design scenario D - SOFC FULL fully relies on SOFCs for all operational requirements.

Consequently, design scenarios 3, C, and D are LNG-only ship designs. An overview of the power split and required fuel storage is provided in Table 1. Fig. 2 shows which grid architectures correspond with the design scenarios. In this study, the grid architecture selection mainly influences the electrical conversion losses. For the reference scenarios, a conventional AC net has been selected as shown in Fig. 2(a). For the full SOFC scenario, a DC architecture is selected, as shown in

Table 1
Overview of installed components and fuel dimensioning for considered design scenarios. AUX = auxiliaries, MAN = manoeuvring.

DS	Design scenario	Installed power split		Fuel tank dimensioning	
		SOFC	GEN	MGO	LNG
1	DG	0%	100% (4 DGs)	All operations DG	–
2	DFG	0%	100% (4 DFGs)	Pilot fuel Range extender	Main operations
3	GG	0%	100% (4 GGs)	–	All operations
A	SOFC AUX	P_{AUX}	Remainder (3 DFGs)	Pilot fuel Range extender	Auxiliaries SOFC Propulsion DFG
B	SOFC MAN	$P_{AUX}+P_{MAN}$	Remainder (3 DFGs)	Pilot fuel Range extender	AUX & MAN SOFC Remainder DFG
C	SOFC CRUISE	$P_{AUX}+P_{PROP}$	Remainder (3 GGs)	–	All operations
D	SOFC FULL	100%	0%	–	All operations

Fig. 2(c). Fewer transformers and switchboards are needed to supply fuel cell power to a DC grid, improving system efficiency and lowering the size, weight, and cost of the system [34]. For the hybrid scenarios, the two architectures are combined, as shown in Fig. 2(b). This makes it possible to avoid conversion losses for DC users, while still relying on off-the-shelf AC components for the main net. An AC–DC conversion efficiency of 96% is assumed while the DC-DC conversion is assumed at 98%.

2.2. Component sizing model

The installed capacity of the power-producing components is already presented in Table 1. An initial battery capacity is estimated assuming conservatively that the total power plant should have the same transient capabilities as dual-fuel gensets. Since the batteries should support energy as well as power supply, the battery capacity is established from both, see Eqs. (1) to (3).

$$E_{BAT,req} = \frac{P_{SOFC,installed}}{2 \cdot T_{trans,SOFC}} - \frac{P_{SOFC,installed}}{2 \cdot T_{trans,ENG}} \tag{1}$$

$$P_{BAT,req} = \left(T_{trans,ENG} - T_{trans,SOFC}\right) \cdot \frac{P_{SOFC,installed}}{T_{trans,ENG}} \tag{2}$$

$$E_{BAT} = \max\left(E_{BAT,req};\ \frac{P_{BAT,req}}{C_{rate}}\right) \tag{3}$$

Where E_{BAT} is the battery capacity, P is the power, and T_{trans} is the transient capability of the power-generating component in percentage of total power per second. The C_{rate} is the rate at which the battery is charged or discharged, where 1C corresponds to discharge in an hour and 2C in two hours. The derivation of this equation can be found in the supplementary materials. The required heat-producing capacity of the boilers $\dot{Q}_{BOIL}$ is sized from the required heat demand and the heat produced by the SOFCs and gensets for every sail mode:

$$\dot{Q}_{BOIL} = \max\left(\dot{Q}^s_{load} - \dot{Q}^s_{ENG} - \dot{Q}^s_{SOFC}\right)_{s=sailmode} \tag{4}$$

Both the battery capacity and boiler capacity will be adapted to the actual requirements of the load profile using the dynamic simulation, which is described in Section 2.4.

The required fuel capacity is estimated using the end-of-life efficiency η_{EOL} of the power plant components and a 10% margin S_{fuel}. The estimation includes MGO and LNG consumption for gensets (also including pilot fuel), SOFCs and boilers. A generalised formulation of the calculation is shown in Eq. (5).

$$E_{fuel} = \left(1 + S_{fuel}\right) \cdot \left(\frac{\frac{P_{component}}{P_{installed}} \cdot E_{max,fuel}}{\eta_{component,EOL}}\right) \tag{5}$$

Where $E_{max,fuel}$ is the energy required of the dedicated fuel to fulfil the range and endurance requirements as derived from the load profile.

The capacity of the various components is combined with an elaborate database of power density and energy density to estimate the required volume and mass of the different components according to Eqs. (6) to (7). The database (see Table 2) is established from literature and supplier data. To ensure the integrity of this dataset, a consistent scope of the needed auxiliary components was essential.

$$V_{component} = \frac{P_{component}}{p_{vol,component}} \tag{6}$$

$$m_{component} = \frac{P_{component}}{p_{grav,component}} \tag{7}$$

2.3. Power plant simulation model

This section describes how the power plant components and the energy management strategy are modelled. Matlab Simulink© is used for the time-domain simulations.

2.3.1. Fuel cell model

Haseltalab et al. [17] used an isothermal plug flow reactor to calculate the current–voltage characteristics and fuel consumption of the SOFC stack for different loads. They modelled the transient response by limiting the rate of change of the stack current. Constant and load-dependent loss terms account for the parasitic consumption of auxiliary components. This model is adapted by including differences in heat loss and fuel utilisation in part-load conditions. Because of a difference in stack temperature, the heat losses cannot be assumed constant. Moreover, SOFC systems are often operated at lower fuel utilisation at part-load in order to feed additional fuel to the burner to ensure sufficient heat supply to the stack. This adaptation makes the net-efficiency curve (see Fig. 3) correspond better with published data of commercial SOFC systems [19]. Additionally, a distinction is made between the allowed current density rate during ramp-up and ramp-down, which is formulated in Eq. (8). Transient SOFC experiments showed a four times higher ramp-down rate (see Table 3), because the temperature change in the cells is more uniform than during ramp-up [37] The heat efficiency is based on supplier data of the available heat in the exhaust stream. Although the heat efficiency is assumed to be constant over its lifetime (see Fig. 3), the delivered heat increases, because more fuel is fed to the SOFC due to the decrease in electrical efficiency. It is assumed that heat can only be recovered up to 100 °C for the hot water and steam net [38], which explains why the heat efficiency is slightly lower than reported by SOFC system manufacturers. The specific emissions of the SOFC are based on literature and reported in supplementary materials.

$$u(t) = \begin{cases} u(t) = \Delta t \cdot R + i(t-1) & \text{if i}' > \text{R} \\ u(t) = -\Delta t \cdot F + i(t-1) & \text{if i}' < \text{F} \\ u(t) & else \end{cases} \tag{8}$$

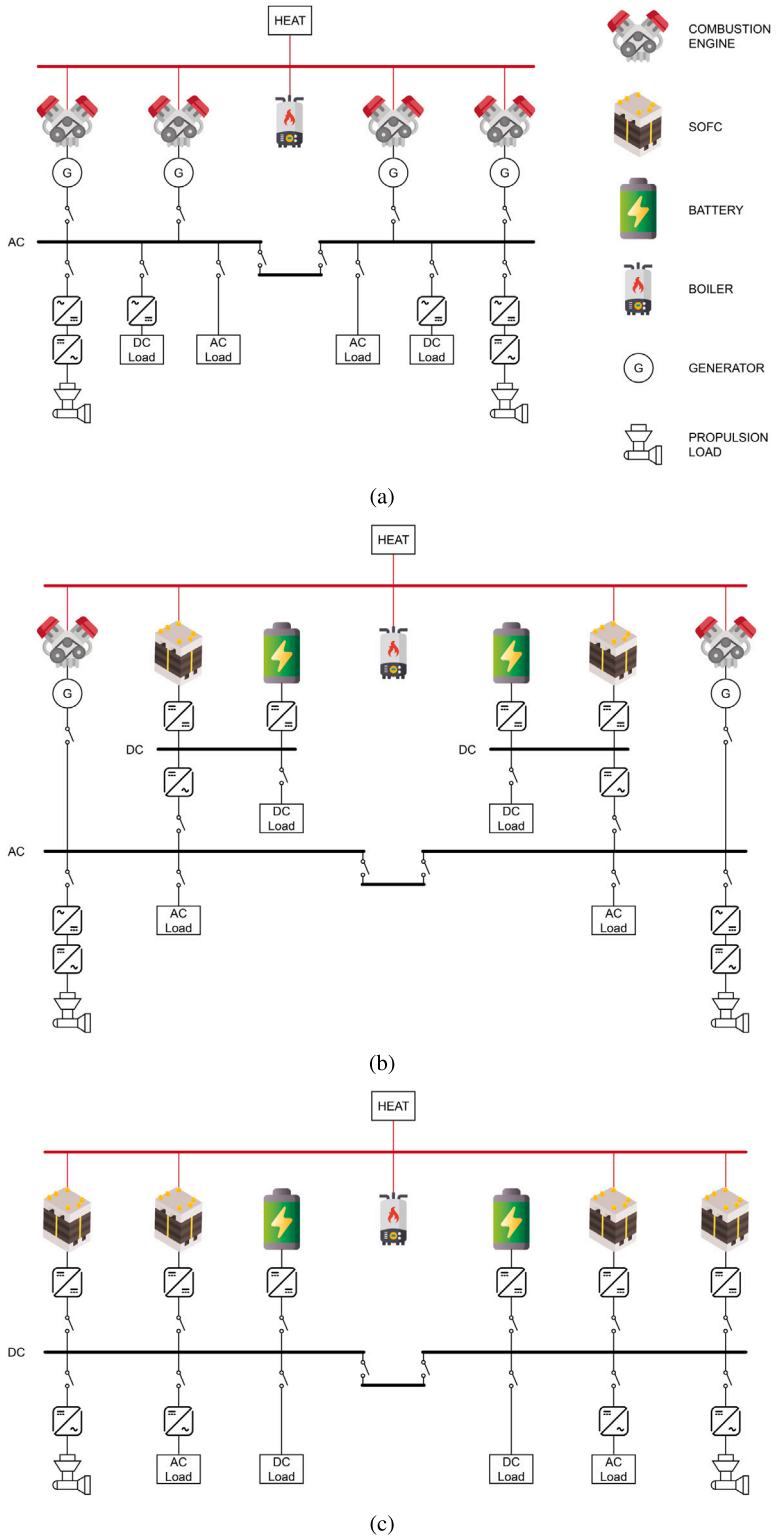

Fig. 2. Grid architectures: (a) AC grid architecture for reference scenarios 1-3; (b) Mixed grid architecture for SOFC scenarios A-C; (c) DC grid architecture for SOFC scenario D.

Where i is the input, u the output, t the time, R the rising slew rate, and F the falling slew rate.

A novel approach is used to include the degradation effects. Decreasing cell voltage reduces the rated power and efficiency at a specific current density. However, when constant power output is required, the current density must be increased along the i-V curve, further decreasing voltage and thus efficiency [39]. Moreover, a rise in current density increases the degradation rate [40]. To incorporate this, a degradation resistance term is added to calculate the power of the fuel cell:

$$P = V_{cell} \cdot I = \left(V_0 - I\left(R + R_{deg}\right)\right) \cdot I \tag{9}$$

Where V_{cell} is the cell voltage, R is the cell resistance, and R_{deg} is the additional resistance due to degradation effects. Solving for the current

Table 2
Used data to estimate component size and weight. The energy density of the fuel also includes storage equipment.

Variable	Component	Fuel	Value	Unit	Source
p_{vol}	SOFC	LNG	15	kW/m^3	[12,35]
p_{grav}	SOFC	LNG	25	kW/ton	[12]
p_{vol}	DG	MGO	45	kW/m^3	[12]
p_{grav}	DG	MGO	60	kW/ton	[12]
p_{vol}	DFG	Both	40	kW/m^3	Wartsilla, MAN, CSI
p_{grav}	DFG	Both	50	kW/ton	Wartsilla, MAN, CSI
p_{vol}	GG	LNG	40	kW/m^3	Same values as DFG
p_{grav}	GG	LNG	50	kW/ton	Same values as DFG
p_{vol}	BOIL	MGO	104	kW/m^3	[9]
p_{grav}	BOIL	MGO	360	kW/ton	[9]
p_{vol}	BOIL	LNG	75	kW/m^3	Alfa Laval
p_{grav}	BOIL	LNG	310	kW/ton	Alfa LAval
e_{vol}	BAT (Li-ion)	–	90	kWh/m^3	[9]
e_{grav}	BAT (Li-ion)	–	80	kWh/ton	[9]
e_{vol}	–	MGO	8200	kWh/m^3	[22]
e_{grav}	–	MGO	8300	kWh/ton	[22]
e_{vol}	–	LNG	3443	kWh/m^3	[36]
e_{grav}	–	LNG	8050	kWh/ton	[36]

Table 3
Used parameters for simulation model.

General	Parameter	Value	Unit
Lower heating value MGO	LHV_{MGO}	42 800	kJ/kg
Lower heating value LNG	LHV_{LNG}	50 000	kJ/kg
CO_2 equivalent methane	CO_2-eq_{CH4}	25	–
Safety margin fuel capacity	S_{fuel}	10%	–
SOFC			
Nominal voltage at BOL	$V_{cell,BOL}$	0.85	V
Nominal voltage at EOL	$V_{cell,EOL}$	0.71	V
Max current change rise	R	2% of P	/min
Max current change fall	F	8% of P	/min
Transient threshold	T_{thold}	0.03%	/min
Transient factor	a_{trans}	1.5	–
Nominal stack lifetime	L_{SOFC}	30 000	h
Genset			
Transient capability on MGO	$T_{trans,MGO}$	2.7% of P	/s
Transient capability on LNG	$T_{trans,LNG}$	1.4% of P	/s
Generator efficiency	η_{gen}	95%	–
Amount of pilot fuel for DFG	p_{DFG}	3%	–
Lower load limit	LL	10%	–
Battery			
Charge efficiency	η_{ch}	90%	–
Discharge efficiency	η_{dis}	95%	–
Max C-rate	C_{rate}	3	–
Initial SOC	SOC_{init}	0.55	–
Upper bound SOC	SOC_{UB}	0.9	–
Lower bound SOC	SOC_{LB}	0.2	–
Safety margin	S_{BAT}	10%	–
Boiler			
Boiler efficiency - MGO	η_{MGO}	85%	–
Boiler efficiency - LNG	η_{LNG}	90%	–
Other			
Converter efficiency DC| DC	$\eta_{DC\|DC}$	98%	–
Inverter efficiency AC|DC	$\eta_{AC\|DC}$	96%	–

I yields,

$$I = \frac{V_0 + \sqrt{4P\left(R + R_{deg}\right) - V_0^2}}{2\left(R + R_{deg}\right)} \tag{10}$$

Load cycles reduce lifetime, while degradation is lower at part-load operation since the SOFC is operated at a lower current density. The load-dependent degradation formulation is retrieved from Abreu-Sepulveda et al. [41], who define the degradation rate as a function of the current density i. The function is fitted to the lifetime projected by the SOFC system manufacturer. The degradation model also detects whether the change rate of the current is above the threshold for transient operation T_{thold}, which adds a multiplication factor a_{trans} to the degradation rate, see Eq. (11).

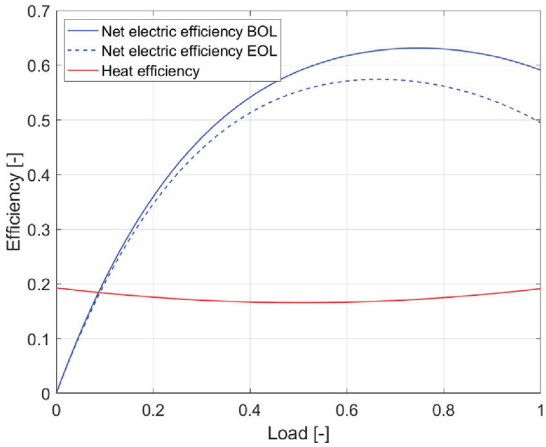

Fig. 3. Net electrical efficiency (DC) and heat efficiency of SOFC system at beginning-of-life and end-of-life. The model of this study is adapted from Haseltalab et al. [17].

$$r_{deg} = a_{trans} \cdot 0.0573 \cdot \exp^{1.25i} \quad \left[\%.\eta_{net}/1000h\right] \tag{11}$$

The degradation rate is integrated over time to find the increase in cell resistance needed for Eq. (10). The state of health SOH is defined from the current cell voltage V_{cell} and the voltage at beginning of life (BOL) and end of life (EOL), see Eq. (12). SOH is usually defined for a constant current density. In this paper, SOH is defined at nominal load P_{nom}, since the current density increases over its lifetime to maintain constant power.

$$SOH = \frac{V_{cell}\left(P_{nom}\right) - V_{cell,EOL}\left(P_{nom}\right)}{V_{cell,BOL}\left(P_{nom}\right) - V_{cell,EOL}\left(P_{nom}\right)} \tag{12}$$

2.3.2. Genset model

The ICE genset is modelled with look-up tables for the efficiency and emissions as a function of the load, see Fig. 4(a) and the supplementary materials respectively. The efficiency and emissions include a constant generator efficiency of 0.95. The dynamic behaviour is captured with a rate limiter (Eq. (8)) on the load and a minimum load of 10% per engine is implemented. The performance depends on the engine type, as defined by the design scenario (Table 1). For the DFG model, 3% pilot fuel is assumed. The allowable load changing rate of gas engines is usually lower than diesel-fuelled engines, see Table 3. For this reason,

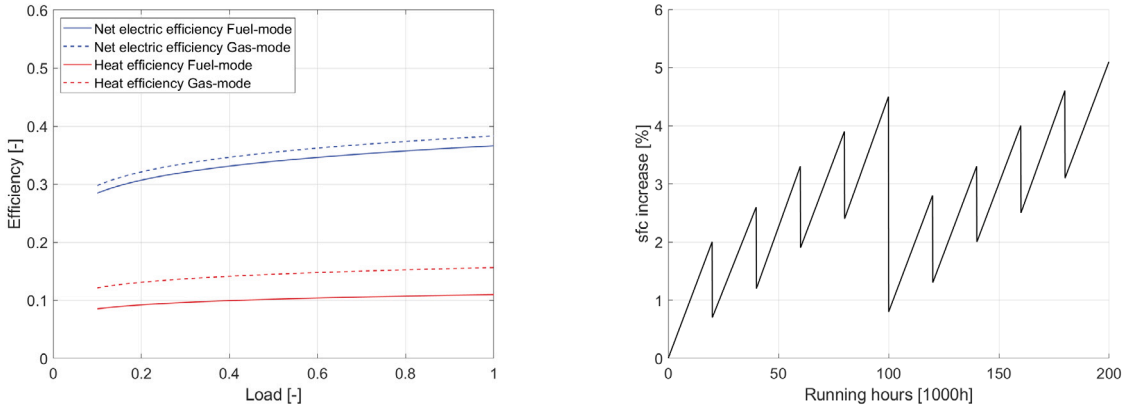

(a) (b)

Fig. 4. Engine performance: (a) Electrical [17] and heat efficiency [42] of gensets for MGO and LNG. Electrical efficiency includes generator efficiency; (b) Increase in specific fuel consumption (sfc) due to wear and fouling of engine components [28]. Improvements are from engine overhauls.

DFGs usually switch to MGO operation during rapid load changes, which is included with the following logic:

$$u = \begin{cases} \text{MGO mode} & \text{if i}' > \text{T}_{trans,LNG} \\ \text{Gas mode} & \text{else} \end{cases} \tag{13}$$

Wear and fouling of engine components is included in the simulation model as an increase in fuel consumption during running hours, as prescribed by Cichowicz et al. [28] in Fig. 4(b).

2.3.3. Battery model

The battery model is based on a power and energy balance model that includes cycle efficiency and degradation effects. The available power is denoted as the current battery capacity times the maximum C_{rate}:

$$P_{BAT,max} = C_{rate} \cdot E_{BAT} \tag{14}$$

This equation neglects the decrease in battery capacity at higher C-rates but this is usually small. The battery degradation is modelled as a superposition of cyclic ageing and calendar ageing. The calendar ageing is independent of the battery current [29]. An algorithm detects whether the battery is in use or idle and applies the cyclic ageing data or the calendar ageing data respectively. Ali et al. [43] proposed a calendar ageing model based on temperature and SOC, substantiated by literature and an extensive experimental campaign. The degradation rate is defined with the derivative of the calendar ageing for NMC Li-ion batteries, as shown in Eq. (15).

$$r_{deg,cal} = 0.03304e^{0.5036SOC} \cdot 385.3e^{-2708T} \cdot 0.51t^{-0.49} \tag{15}$$

Where T is the temperature in Kelvin and t is the time in days. The degradation due to cycling is based on a multi-year study for 18 650 commercial battery cells [44]. The equivalent full cycles for 20% capacity reduction are formulated as a function of the depth of discharge (DOD) and the C_{rate}, as shown in Table 4. The equivalent cycles are calculated with the rainflow algorithm, which is often used for battery degradation with varying DODs [45]. Finally, the capacity degradation is estimated at every timestep by superposition of the degradation rate for calendar ageing and cycle effects. This is used to estimate the number of required battery replacements.

2.3.4. Boiler model

Three boiler models are implemented: oil-fired, gas-fired, and dual-fuel boiler, dependent on the bunker fuels in the dedicated design scenario (see Table 1). The boiler is modelled as an instantaneous heat source supplying the difference between the load and the heat-producing components, as defined in Eq. (16).

Table 4
Number of cycles in battery life for depth of discharge and charge rates [44].

DoD	Cycles in battery life			
	0.5C	1C	2C	3C
0.2	2127	2540	–	–
0.6	1634	1654	–	–
1	429	429	739	571

The heat efficiency and specific emissions are assumed to be load-independent, which can be justified because the boilers are only responsible for a minimal share of fuel consumption and ship emissions. Furthermore, no load transients are applied to the boiler.

$$\dot{Q}_{BOIL} = \dot{Q}_{load} - \dot{Q}_{ENG} - \dot{Q}_{SOFC} \tag{16}$$

2.3.5. Energy management strategy

The SOC-based energy management strategy has been adapted from Ünlübayir et al. [46] and is shown in Fig. 5(a). It has been implemented to divide the load over the SOFCs, gensets and batteries. The hierarchical sequence of the control system prioritises the SOFC, followed by the gensets, with the battery as the third priority. A low-pass filter is applied to the load of the SOFC system. It only passes signals below the cut-off frequency, removing rapid load demand changes. The cut-off frequency is determined based on the transient capabilities of the SOFC and gensets and implemented with transfer function (17).

$$T(s) = \frac{1}{1 + \frac{1}{\omega_0}} \tag{17}$$

The SOFC load is also limited to the installed power of the SOFCs and the remaining higher frequency signal is the resulting load for the gensets (see Eq. (18)). The SOFC model and genset model include the transient behaviour of both components. The actual produced power is compared with the load and the difference is requested from the batteries (see Eq. (19)). The load is artificially increased or decreased to attain the desired SOC for the battery. The initial and target value is set at 0.55, giving the greatest flexibility for discharging or charging the battery at any specific moment. The load is increased with Eq. (20), increasing proportionally with the deviation from the target SOC. Meanwhile, a double hysteresis control has been implemented to prevent rapid cycling of the SOFC around the charge limits of the battery. For instance, for low SOC, the battery starts charging at SOC_{L1} and stops charging at SOC_{L2}. Fig. 5(b) demonstrates the power distribution between the SOFCs, the engines, and batteries during berthing, manoeuvring and cruising for design scenario SOFC MAN. The SOFC

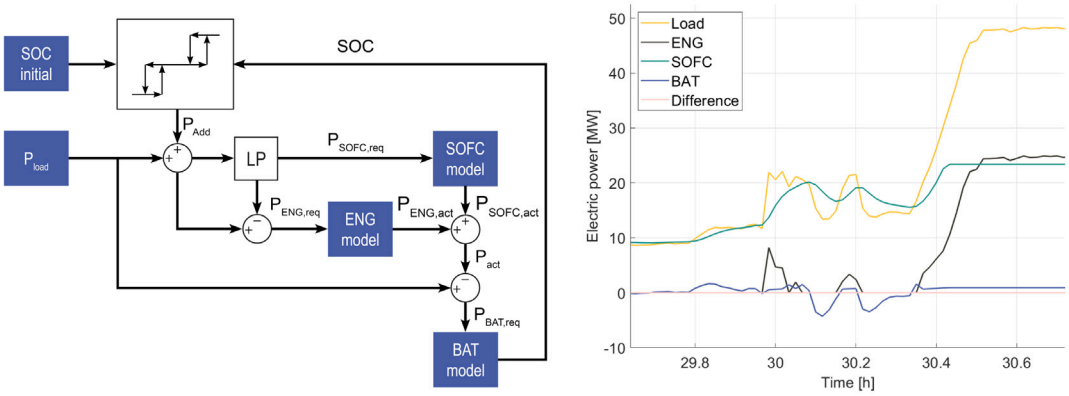

(a) (b)

Fig. 5. Control of the power plant: (a) Energy management strategy; (b) Demonstration of energy management strategy during short interval of operational profile for design scenario B - SOFC MAN.

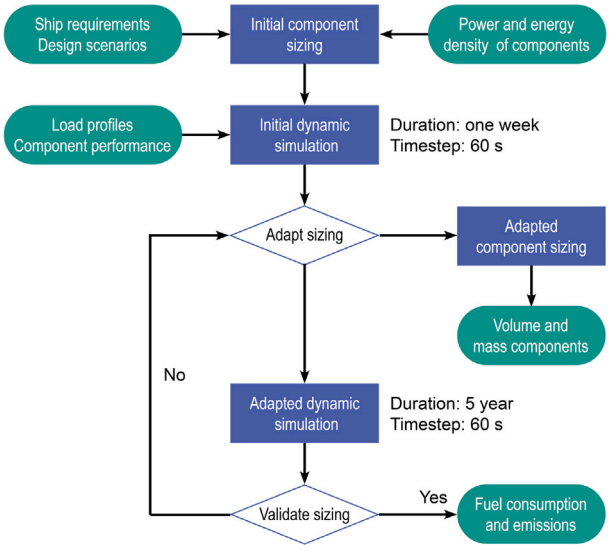

Fig. 6. Flowsheet of simulation steps including timestep and duration.

(green) slowly follows the load up to the maximum installed power, and is compensated by the battery (blue). The gensets (black) are only used when needed and supply power above the installed power limit of the SOFC.

$$P_{ENG,req} = P_{load} + P_{add} - P_{SOFC,req} \tag{18}$$

$$P_{BAT,req} = P_{load} + P_{add} - P_{SOFC,act} - P_{ENG,act} \tag{19}$$

$$P_{add}(t) = \left(SOC_{L2} - SOC(t)\right) \cdot a_{SOC} \cdot E_{BAT} \cdot C_{rate} \tag{20}$$

The recoverable heat produced from SOFCs and gensets is compared with the heat load and complemented by firing the boilers. Excess heat is expelled from the ship through the exhaust stream.

2.4. Adaptation of battery and boiler components

The initial sizing of both the battery and the boiler is necessary to run the simulation. Subsequently, the simulation outcomes are used to validate the precision of these estimations. The required power and energy capacity of the battery and boiler are compared with the constraints imposed by the installed components (Eqs. (21) and (23) for the battery). This comparison yields a utilisation ratio u, which is used to resize the battery, including a 10% safety margin as shown in Eq. (24). A similar formulation is used to resize the boiler.

$$u_{SOC,LB} = \frac{\min\left(SOC(t)\right) - SOC_{target}}{SOC_{LB} - SOC_{target}} \tag{21}$$

$$u_{SOC,LB} = \frac{\min\left(P_{BAT}(t)\right)}{E_{BAT,init} \cdot C_{rate}} \tag{22}$$

$$u_{BAT} = \max\left(u_{SOC,LB};\ u_{SOC,UB};\ u_{P,LB};\ u_{P,UB}\right) \tag{23}$$

$$E_{BAT,adapted} = (1 + S_{BAT}) \cdot E_{BAT,init} \cdot u_{BAT} \tag{24}$$

Table 5
Main particulars of ship used for case study.

	Cruise ship	Unit
Length	292	m
Width	38.3	m
Draft	8.7	m
Passengers	4000	–
Crew	1600	–
Installed power	75 000	kW
-Auxiliaries	13 125	kW
-Manoeuvring	23 400	kW
-Main operations	38 400	kW

3. Results

The component sizing model and power plant simulation model are applied to a cruise ship. The main particulars and load profiles are supplied by a shipyard and scaled to the size of a fictive cruise ship for confidentiality purposes using the cruise ship database presented in van Veldhuizen [15]. Its main particulars are summarised in Table 5. The load profile consists of a week of cruise operation with daily port calls. Yearly the ship performs 48 cruise travels and two transatlantic journeys. First, one week is simulated to assess the initial sizing of the battery and boiler, followed by a five-year simulation to fully account for the degradation effects within one dry docking maintenance interval. All time-domain simulations use a step size of 60 s and Fig. 6 shows an overview of the inputs, simulation order, and outputs. The applied component models, energy management strategy and degradation formulations provide a relatively low-computational model. Five years of power plant operation are simulated in 10.4 h.

3.1. Volume and mass of power plant

This section contains the results of the component sizing model. Figs. 7(a) and 7(c) show that increasing the number of installed SOFC

Table 6
Reduction in battery capacity with respect to initial estimation.

DS	Design scenario	Initial BAT capacity [kWh]	Adapted BAT capacity [kWh]	BAT reduction
A	SOFC AUX	4210	2200	48%
B	SOFC MAN	7506	5465	27%
C	SOFC CRUISE	18 321	10 444	43%
D	SOFC FULL	24 059	7736	68%

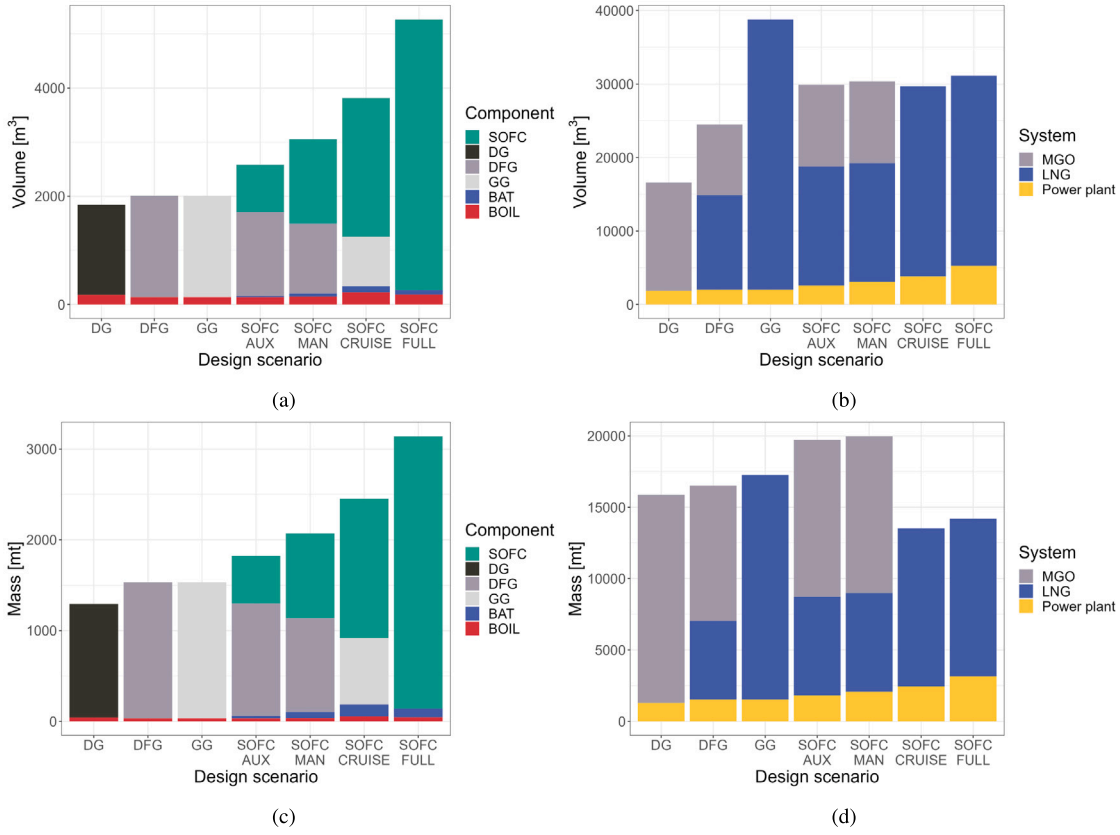

Fig. 7. Sizing of power plant after adapting boiler and battery capacity: (a) Volume of power plant; (b) Volume of power plant and fuel storage; (c) Mass of power plant; (d) Mass of power plant and fuel storage. The left graphs form the yellow part of the right graphs.

systems requires more space and mass for power-producing components due to a lower power density, which is similar to results presented by Li et al. [23]. However, when including volume for fuel storage, the volume increase diminishes for higher installed SOFC power, see Fig. 7(b). The power plant of SOFC FULL is 162% larger than the DFG power plant, while the total volume for the power plant and fuel storage is 27% higher. The power plant of SOFC FULL is 104% heavier compared to DFG, but when fuel storage is included the weight is 14% less. This is due to the high conversion efficiency of SOFCs, which reduces the required fuel storage size to meet range requirements. It is also interesting to note that all SOFC scenarios have a smaller power plant than a fully LNG-powered ship using solely gas engines. Moreover, the mass of the total power plant of design scenarios SOFC CRUISE and SOFC FULL is lower than the conventional options as shown in Fig. 7(d), due to the weight of MGO.

The presented results are generated using the adapted battery and boiler capacity (see Section 2.4). The change in battery capacity is shown in Table 6. Large reductions in battery capacity are realised using dynamic simulations. This highlights the importance of a detailed power plant simulation model to prevent over or under-dimensioning of auxiliary components. The change in mass and volume of the power plant was minor, as the boiler capacity partially offset the alteration, and the boiler and battery constitute only a small portion of the overall power plant.

3.2. Power and energy balance

The first week of the adapted simulation is visualised in Figs. 8 and 9. Fig. 8 illustrates the power output of the components. In 8(a) and 8(b), the SOFCs follow the load and gensets supplement power beyond the SOFCs' capacity. For design scenario SOFC CRUISE, the gensets are required intermittently during significant fluctuations in propulsion demand. The variation in battery power is much lower when the SOFCs are only used for the auxiliary power, which corresponds with the smallest required battery capacity of design scenario SOFC AUX in Table 6. Figs. 8(c) and 8(d) clearly illustrate a distinction between the load and the produced power. These represent the power conversion losses, which are lower for design scenario SOFC FULL, because a full DC grid is used.

Notably, the largest peaks in battery power occur when the ship slows down, storing power in the batteries, despite the SOFCs' allowable ramp-down current rate being four times higher than the ramp-up limit. The used load profile is derived from an engine-operated ship and is managed accordingly. Reducing the speed more gradually could

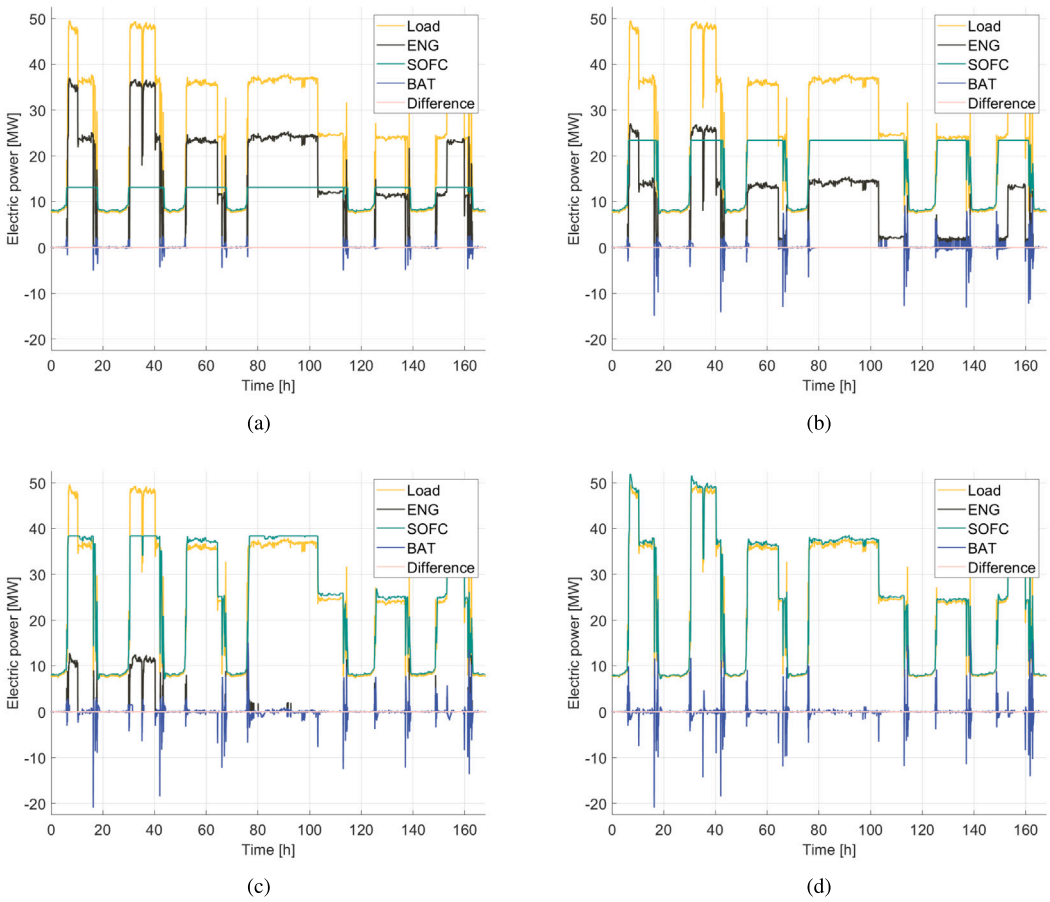

Fig. 8. Delivered power by components for SOFC scenarios during the first week of the simulation: (a) Design scenario SOFC AUX; (b) Design scenario SOFC MAN; (c) Design scenario SOFC CRUISE; (d) Design scenario SOFC FULL.

lower the required battery capacity. The implications of changing ship requirements are discussed extensively in Section 4.1.

When the transient capability is insufficient to meet a change in the load profile, batteries provide additional power. As can be seen in Fig. 9(a), batteries are consistently used for load-smoothing, with significant demand only during changes in ship speed. Consequently, battery cycling is limited and battery lifetime is preserved. The effectiveness of the energy management strategy is evident, SOC of the batteries remains mostly between 0.4 and 0.6.

The heat load and production are shown in Fig. 9(b). Although the full boiler capacity is rarely used, a significant amount of boiler capacity is needed throughout the cruise operation, as the SOFCs and gensets do not generate enough heat to fulfil the load profile. Occasionally, there is a large amount of unused heat, but it is not consistent enough to justify additional heat recovery systems.

For all simulated design scenarios, the modelled power plant fully meets the electrical and heat load profile.

3.3. Degradation effects

The degradation speed of SOFCs and batteries varies with loading and cycling conditions across the design scenarios. Table 7 and Fig. 10 show the degradation of these components after five years. The remaining SOH of the SOFCs is 0.47 for design scenario SOFC FULL, which is the highest among the design scenarios. This is the case because the degradation is a function of the current density (see Eq. (11)) and the SOFCs are mostly operated at part-load. Although the load of SOFC AUX is more stable, the remaining SOH of 0.08 is the lowest for this scenario. Apparently, the load-dependent degradation dominates the consequences of transient operation. For all design scenarios, the observed degradation of SOFCs accelerates over their lifetime, because the current density gradually increases to maintain the rated power. The degradation analysis reveals that all scenarios finish five years of operation before stack replacement, although thermal cycles are not considered. Implementing additional power capacity, as in the SOFC FULL design scenario, can extend the overall system's lifespan by operating the stacks at a lower current.

The battery requires replacement 0.9 to 1.65 times within five years across different design scenarios. This exceeds expectations, as marine battery suppliers typically claim a lifespan of 5 to 10 years, corresponding to 2000 to 3000 equivalent cycles [47]. However, this holds only for low C_{rate}, while the SOFC system's slow transient response needs high battery power output. Installing additional batteries could reduce the required C_{rate}, therefore extending the battery's cycle life, although this increases volume and cost. The fastest degradation occurs in the SOFC MAN design scenario, due to high C_{rate} and large DOD during manoeuvring operations. The SOFC CRUISE scenario reaches the five-year operational interval.

3.4. Fuel consumption and emissions

Fig. 11 shows the fuel efficiency and consumption across the design scenarios during five years of operation. For design scenarios

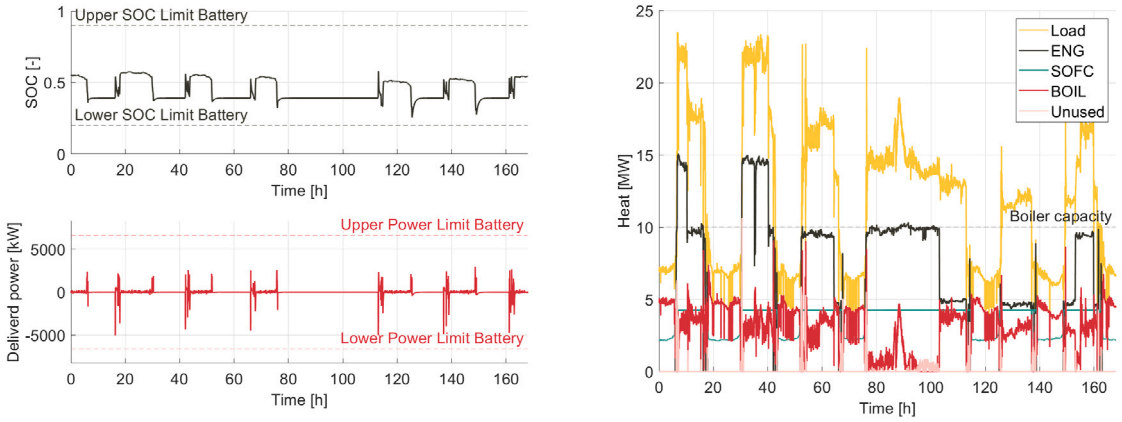

(a) (b)

Fig. 9. Design scenario SOFC AUX during the first week of simulation: (a) Battery operation; (b) Heat balance.

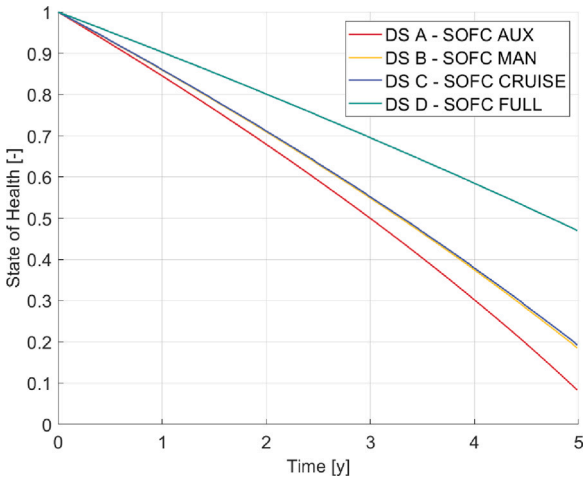

Fig. 10. State of health of SOFC stacks for different design scenarios during 5-year simulation.

Table 7
Overview of SOFC and battery degradation after 5-year simulation.

DS	Design scenario	SOFC SOH	BAT replacements
A	SOFC AUX	0.08	1.49
B	SOFC MAN	0.19	1.65
C	SOFC CRUISE	0.19	0.90
D	SOFC FULL	0.47	1.10

DFG, SOFC AUX, and SOFC MAN, there is some MGO consumption as pilot fuel. The average fuel efficiency increases with greater use of SOFCs. Nevertheless, the fuel consumption is higher for the fully SOFC-powered ship. This is the case because all SOFCs are operated on the same load. With a higher installed SOFC power, especially in berth, this leads to a significantly lower conversion efficiency. This limitation of the simulation model will be further discussed in Section 4.2. Overall, all four SOFC scenarios result in a major fuel consumption reduction, compared to the reference scenarios. Although the boiler's fuel consumption slightly increases with more SOFC usage, this is negligible compared to the gains in electrical efficiency, as shown in 11(b).

Fig. 12 illustrates the GHG, NO_X, SO_X, PM and CO emissions for the design scenarios during 5 years of operation. WTT emissions are also included if reliable data was available. Fig. 12(a) shows that adapting to LNG only reduces GHG emissions by a little compared with MGO-fuelled gensets. Although the WTT emissions are lower for LNG, methane slip in current engines is high, especially at part-load conditions. Using SOFCs solely for auxiliary loads significantly reduces GHG emissions. Additionally, the reduction in fuel consumption leads to a decrease in WTT emissions. However, in design scenario SOFC FULL, GHG emissions increase, corresponding with the rise in fuel consumption. Compared with diesel generators, all SOFC scenarios result in a GHG reduction of over 30%, complying with the IMO target to reduce GHG emissions by 30% by 2030 IMO [6]. None of the SOFC scenarios reach the 80% reduction target set for 2040. Renewable fuels could be applied to further decrease GHG emissions.

LNG-fuelled gensets emit significantly less NO_X and particularly SO_X emissions compared to MGO-fuelled gensets, although dual-fuel and gas engines produce higher PM and CO emissions. All pollutant emissions of SOFCs are minimal, thus the NO_X, SO_X, PM and CO emissions in design scenarios SOFC AUX, SOFC MAN and SOFC CRUISE mainly originate from the gensets. In design scenarios SOFC CRUISE and SOFC FULL most pollutant emissions are eliminated.

4. Discussion

This section reflects on the validity of the simulation model. First, potential changes in the ship's requirements for an SOFC ship are discussed. Subsequently, the limitation of the model concerning part-load operation is addressed. Finally, the applicability of the model to other ship types and load profiles is assessed.

4.1. Range and installed power requirements

The analysis of various design scenarios revealed that accommodating the proposed power plant would be challenging without sacrificing valuable space. Introducing low-power-density technologies, like SOFCs, and low-energy-density fuels, often stored in large cryogenic tanks, leads to a reevaluation of ship design requirements. Conventional ships typically have tank storage designed for high range and endurance, yet in practice, much of this space remains unused. In this study, it was found that only 20% to 60% of the stored fuel across the design scenarios, as estimated based on a 20-day endurance criterion, was required to fulfil the operational profile. The sensitivity analysis in Fig. 13 shows that the volume of the whole power plant strongly reduces for lower endurance requirements.

Moreover, maximum installed power requirements are often based on redundancy needs. For example, with four engines divided between

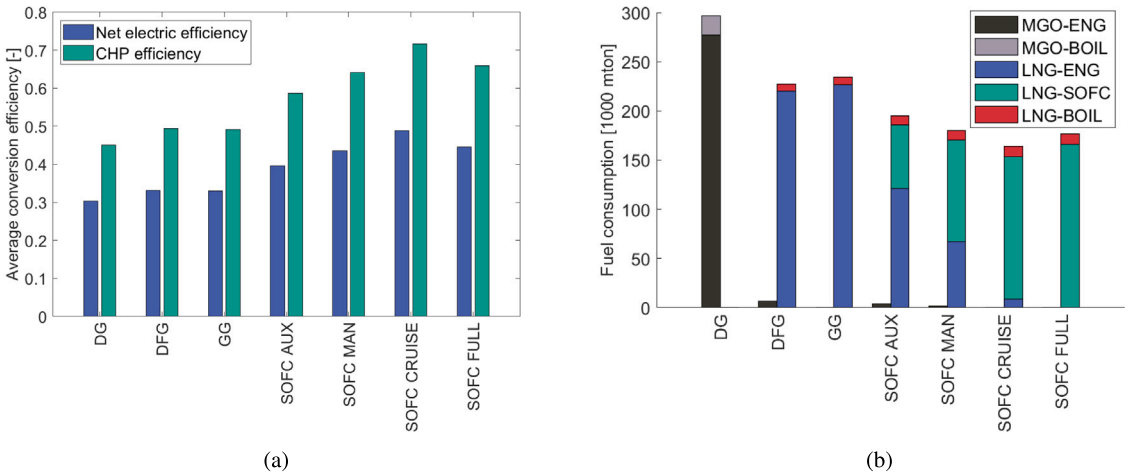

Fig. 11. Fuel efficiency (a) and fuel consumption (b) of simulated power plants for five years of operation.

two main vertical zones, losing one zone still requires sufficient power for a safe return to port. Fuel cells, when installed in a decentralised manner, can enhance redundancy and potentially reduce the overall installed power requirements. Additionally, the battery SOC approached its limit during slowdown phases, as SOFCs temporarily produced excess power. To address this, reducing speed earlier and more gradually could decrease the necessary battery capacity.

In this study, operational requirements were kept constant to ensure a fair comparison of design scenarios. However, aligning ship requirements more closely with the operational profile and power plant components could significantly reduce the size and cost of the power plant. This approach, though, would diminish the operational flexibility of the ship. Ship owners must carefully consider whether reduced ship requirements would render the vessel less versatile for varying scenarios.

4.2. Advanced energy management

In scenario D, where only SOFCs are installed, fuel efficiency is lower compared to scenario C, which has just enough power to fulfil all main operations. This inefficiency arises because all SOFCs operate at the same load. Higher installed power at part-load results in lower conversion efficiency (Fig. 3), particularly at berth, where the electrical load represents only 10% to 15% of the installed power. Although these results align with the simulation model, this is unlikely to reflect real power plant operations. To avoid low conversion efficiency at low loads, a fully SOFC-powered plant would likely control groups of SOFC modules, turning them on or off as needed. Optimising this control strategy is an interesting area for future research, focusing on fuel consumption, emissions, and lifetime conservation. However, cold starts take up to 24 h and thermal cycles impact lifespan significantly [48]. Alternatively, groups of SOFC modules could run on hot stand-by, avoiding thermal cycles but consuming some parasitic fuel to maintain temperature. Consequently, such a control strategy would require complex optimisation with many decision variables, warranting a separate study. Once developed, this control could be implemented in the power plant simulation.

4.3. Applicability of simulation model

Since the simulations are executed for a specific ship, the transferability of the results is questionable. Nevertheless, the scientific relevance lies in the method, which can be directly applied to other cruise ships. Cruise ships are investigated due to their significant thermal load and relatively high and constant auxiliary load. However, the developed framework and simulation model are adaptable to other ship types. The study's findings indicate that heat recovery does not offer improvements over gensets, suggesting that high thermal demand is not a prerequisite for efficient SOFC operation. Nevertheless, other ship types differ in their load profile. For example, dredgers have highly variable auxiliary load profiles and frequently use flywheels for energy storage. Such components can be incorporated into the simulation framework, though the results should be revalidated. The research further demonstrated that the required battery capacity and SOFC degradation are smaller when operating under a relatively constant load profile, as in scenario SOFC AUX. Therefore, ship applications with a stable load profile, such as deep-sea cargo and container ships are recommended for SOFC integration.

The study also shows that significant emission reductions are achievable with LNG-fuelled SOFCs. Nevertheless, LNG remains a fossil fuel with considerable carbon emissions. The marine industry is exploring several alternative fuels, such as methanol, hydrogen, and ammonia, as green alternatives. These could be integrated into the simulation framework if reliable sizing, efficiency, and emission data of SOFCs fuelled with alternative fuels are available. This study excluded these fuels due to the lack of such data.

5. Conclusion

The performance of a marine SOFC power plant is evaluated on size, weight, fuel consumption, and emissions. Four LNG-fuelled SOFC design scenarios are compared using an iterative component sizing and time-domain power plant model. The power plant components (SOFC, gensets, battery, and boilers) and their degradation are modelled in Matlab Simulink© and an SOC-based control strategy is used to allocate the requested power. A large cruise ship serves as case study, using five years of electrical and heat load profiles. The applied iterative sizing and dynamic simulation method emphasises the importance of time-domain simulation for adequate power plant sizing. The battery capacity was reduced by 27% to 68% while the boiler capacity had to be increased. Simulations confirm that the degradation rate of the SOFC system depends greatly on its operation. The remaining state of health was lowest for design scenario SOFC AUX, meaning the degradation is more heavily influenced by the load level than the fuel cell's modulation for the evaluated load profile.

Installing more SOFCs strongly increases the size and mass of the power installation. However, this increase is partly offset by a reduction in fuel storage due to the high conversion efficiency. This becomes most relevant for ships with high range and endurance requirements. Compared with the reference scenarios, the SOFC scenarios increase fuel efficiency by 19% to 59%. All design scenarios result in significant emission reductions. Design scenario SOFC AUX minimally impacts

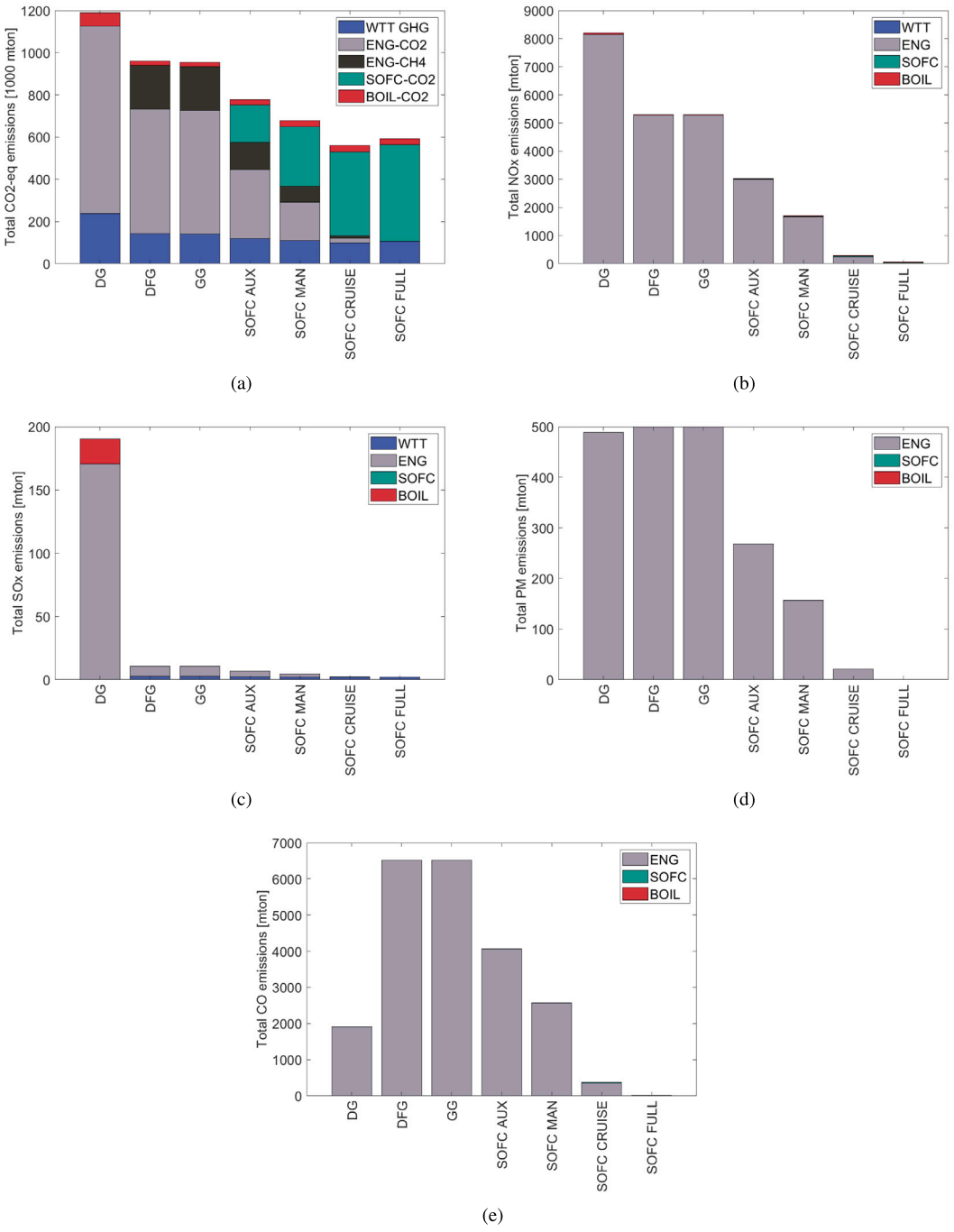

Fig. 12. Greenhouse gas and pollutant emissions of simulated power plants for defined design scenarios: (a) GHG emissions; (b) NO_X emissions; (c) SO_X emissions; (d) PM emissions; (e) CO emissions.

capital costs and power plant design, making it economically advantageous. Compared with dual-fuel gensets, a 21% GHG reduction and 38% to 46% reduction across the reported pollutants is obtainable with only 17.5% of installed SOFC power. This is possible because of improved fuel efficiency and methane slip reduction. Moreover, using the SOFCs mainly for the more stable auxiliary load limits the required battery capacity. Design scenario SOFC MAN has operational advantages. With 31% SOFC power, it is possible to operate at low speeds in low-emission zones while reducing GHG emissions by 33% and pollutants with 60% to 70%. Using SOFCs for all the main cruise operations is recommended from an environmental perspective, resulting in 49% GHG reduction and pollutants by 94% to 96% at 51% installed SOFC power. Pollutants can be eliminated to negligible levels with a fully SOFC-powered ship, although an advanced energy management strategy is required to ensure high conversion efficiency at part-load.

The paper shows that large emission reduction is possible even without fully optimising the operation of the SOFC modules. All considered SOFC scenarios meet the IMO target to reduce GHG emissions by 30% by 2030, and more importantly, with available technology and fuel infrastructure. To further decrease emissions for future emission targets, the SOFC power plant model should be extended for renewable fuels and grouped modulation control should be implemented for optimal fuel conversion at part-load. An energy management strategy that optimises towards fuel consumption, emissions, and lifetime could be used to improve component operation. Furthermore, only four SOFC scenarios are defined in this study. An optimal architecture could be

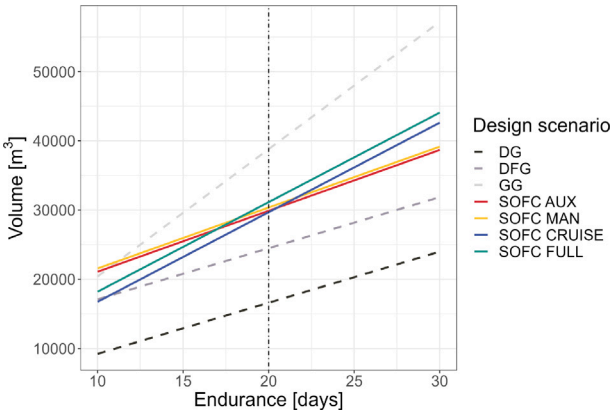

Fig. 13. Sensitivity analysis of ship endurance on and volume of the power plant and fuel storage combined.

assessed from a wide range of hybrid configurations by combining the power plant volume, weight, fuel consumption, and emissions into an objective function.

CRediT authorship contribution statement

B.N. van Veldhuizen: Writing – original draft, Methodology, Formal analysis, Conceptualization. **L. van Biert:** Writing – review & editing, Methodology, Conceptualization. **C. Ünlübayir:** Writing – review & editing, Methodology. **K. Visser:** Supervision, Funding acquisition. **J.J. Hopman:** Supervision. **P.V. Aravind:** Supervision.

Declaration of competing interest

The authors declare that they have no known competing financial interests or personal relationships that could have appeared to influence the work reported in this paper.

Acknowledgements

This research is supported by the European Nautilus Project (grant number 861647), which aims at developing, evaluating, and validating a highly efficient and dynamic integrated SOFC fuelled by LNG for long-haul passenger ships. The authors acknowledge the use of computational resources of DelftBlue supercomputer, provided by Delft High Performance Computing Centre.

Appendix A. Supplementary data

Supplementary material related to this article can be found online at https://doi.org/10.1016/j.enconman.2024.119477.

Data availability

The model parameters, used matlab and simulink models, and output data for this article will be published on data repository'4TU research data'.

References

[1] IEA. International shipping. 2023, URL https://www.iea.org/energy-system/transport/international-shipping.
[2] SEA-LNG. Global fleet - SEA-LNG. 2024, URL https://sea-lng.org/why-lng/global-fleet/.
[3] Comer B, Beecken J, Vermeulen R, Sturrup E, Paschinger P, Osipova L, et al. Fugitive and unburned methane emissions from ships. Technical report, 2024, URL www.theicct.org.
[4] Van Hoecke L, Laffineur L, Campe R, Perreault P, Verbruggen S, Lenaerts S. Challenges in the use of hydrogen for maritime applications. In: Energy and environmental science, vol. 14, no. 2, 2021, p. 815–43.
[5] IMO. Rules on ship carbon intensity and rating system enter into force. 2022, URL https://www.imo.org/en/MediaCentre/PressBriefings/pages/CII-and-EEXI-entry-into-force.aspx.
[6] IMO. Revised GHG reduction strategy for global shipping adopted. 2023, URL https://www.imo.org/en/MediaCentre/PressBriefings/pages/Revised-GHG-reduction-strategy-for-global-shipping-adopted-.aspx.
[7] IMO. Nitrogen oxides (NOx) – Regulation 13. 2020, URL http://www.imo.org/en/OurWork/Environment/PollutionPrevention/AirPollution/Pages/Nitrogen-oxides-(NOx)----Regulation-13.aspx.
[8] Elkasfas A, Rivarolo M, Gadducci E, Magistri L, Massardo A. Fuel Cell Systems for Maritime: A Review of Research and Perspectives. Processes 2023;11(97).
[9] Baldi F, Moret S, Tammi K, Maréchal F. The role of solid oxide fuel cells in future ship energy systems. Energy 2020;194:116811. http://dx.doi.org/10.1016/j.energy.2019.116811.
[10] Selvam K, Komatsu Y, Sciazko A, Kaneko S, Shikazono N. Thermodynamic analysis of 100% system fuel utilization solid oxide fuel cell (SOFC) system fueled with ammonia. Energy Convers Manage 2021;249:114839. http://dx.doi.org/10.1016/J.ENCONMAN.2021.114839.
[11] Rivarolo M, Rattazzi D, Magistri L, Massardo A. Multi-criteria comparison of power generation and fuel storage solutions for maritime application. Energy Convers Manage 2021;244:114506. http://dx.doi.org/10.1016/J.ENCONMAN.2021.114506.
[12] van Veldhuizen B, van Biert L, Aravind PV. Solid oxide fuel cells for marine applications. Int J Energy Res 2023. http://dx.doi.org/10.1155/2023/5163448.
[13] Fuel Cell Energy. 250 kW Fuel Cell Spec Sheet. 2022, URL https://go.fuelcellenergy.com/hubfs/SolidOxideFuelCellSpecSheet.pdf.
[14] Baldi F, Ahlgren F, Nguyen T, Thern M, Andersson K. Energy and exergy analysis of a cruise ship. Energies 2018;11(10):2508. http://dx.doi.org/10.3390/en11102508, URL http://www.mdpi.com/1996-1073/11/10/2508.
[15] van Veldhuizen B. Fuel cell systems applied in expedition cruise ships - A comparative impact analysis. Technical report, Delft University of Technology; 2020.
[16] Rivarolo M, Rattazzi D, Magistri L. Best operative strategy for energy management of a cruise ship employing different distributed generation technologies. Int J Hydrog Energy 2018;43(52):23500–10. http://dx.doi.org/10.1016/j.ijhydene.2018.10.217.
[17] Haseltalab A, van Biert L, Sapra H, Mestemaker B, Negenborn R. Component sizing and energy management for SOFC-based ship power systems. Energy Convers Manage 2021;245:114625. http://dx.doi.org/10.1016/J.ENCONMAN.2021.114625.
[18] Winnes H, Fridell E. Particle emissions from ships: Dependence on fuel type. J Air Waste Manage Assoc 2009;59(12):1391–8. http://dx.doi.org/10.3155/1047-3289.59.12.1391.
[19] Gandiglio M, Marocco P, Nieminen A, Santarelli M, Kiviaho J. Energy and environmental performance from field operation of commercial-scale SOFC systems. Int J Hydrog Energy 2024;85:997–1009. http://dx.doi.org/10.1016/j.ijhydene.2024.08.332.
[20] Sapra H, Stam J, Reurings J, van Biert L, van Sluijs W, de Vos P, et al. Integration of solid oxide fuel cell and internal combustion engine for maritime applications. Appl Energy 2021;281:115854. http://dx.doi.org/10.1016/j.apenergy.2020.115854.
[21] Sugihara S, Iwai H. Measurement of transient temperature distribution behavior of a planar solid oxide fuel cell: Effect of instantaneous switching of power generation and direct internal reforming. J Power Sources 2021;482. http://dx.doi.org/10.1016/j.jpowsour.2020.229070.
[22] van Biert L, Godjevac M, Visser K, Aravind P. A review of fuel cell systems for maritime applications. J Power Sources 2016;327(February 2018):345–64. http://dx.doi.org/10.1016/j.jpowsour.2016.07.007.
[23] Li C, Wang Z, Liu H, Guo F, Li C, Xiu X, et al. Energy and configuration management strategy for solid oxide fuel cell/engine/battery hybrid power system with methanol on marine: A case study. Energy Convers Manage 2024;307. http://dx.doi.org/10.1016/j.enconman.2024.118355.
[24] Pina E, van Veldhuizen B, Marechal F, Herle J. A comparative techno-economic assessment of alternative fuels in SOFC systems for cruise ships. In: ECS transactions. 2023, p. 2459–72. http://dx.doi.org/10.1149/11106.2459ecst.
[25] Kistner L, Schubert FL, Minke C, Bensmann A, Hanke-Rauschenbach R. Techno-economic and environmental comparison of internal combustion engines and solid oxide fuel cells for ship applications. J Power Sources 2021;508:230328. http://dx.doi.org/10.1016/J.JPOWSOUR.2021.230328.

[26] Alenazey F, Alyousef Y, Alotaibi B, Almutairi G, Minakshi M, Cheng CK, et al. Degradation behaviors of solid oxide fuel cell stacks in steady-state and cycling conditions. Energy Fuels 2020;34(11):14864–73. http://dx.doi.org/10.1021/ACS.ENERGYFUELS.0C02920.

[27] Yang C, Guo R, Jing X, Li P, Yuan J, Wu Y. Degradation mechanism and modeling study on reversible solid oxide cell in dual-mode — A review. Int J Hydrog Energy 2022;47(89):37895–928. http://dx.doi.org/10.1016/j.ijhydene.2022.08.240.

[28] Cichowicz J, Theotokatos G, Vassalos D. Dynamic energy modelling for ship life-cycle performance assessment. Ocean Eng 2015;110:49–61. http://dx.doi.org/10.1016/j.oceaneng.2015.05.041.

[29] Redondo-Iglesias E, Venet P, Pelissier S. Calendar and cycling ageing combination of batteries in electric vehicles. Microelectron Reliab 2018;88–90:1212–5. http://dx.doi.org/10.1016/J.MICROREL.2018.06.113.

[30] Löffler C, Kopka T, Geertsma R, Polinder H, Coraddu A. Optimizing energy management for full-electric vessels: a health-aware approach with hydrogen and diesel employing equivalent consumption minimization strategy. In: 2023 IEEE transportation electrification conference and expo. IEEE; 2023, p. 1–8. http://dx.doi.org/10.1109/ITECAsia-Pacific59272.2023.10372270.

[31] Haseltalab A, Negenborn RR. Model predictive maneuvering control and energy management for all-electric autonomous ships. Appl Energy 2019;251. http://dx.doi.org/10.1016/j.apenergy.2019.113308.

[32] Oubelaid A, Khosravi N, Belkhier Y, Taib N, Rekioua T. Health-conscious energy management strategy for battery/fuel cell electric vehicles considering power sources dynamics. J Energy Storage 2023;68:107676. http://dx.doi.org/10.1016/J.EST.2023.107676.

[33] Bessekon Y, Zielke P, Wulff AC, Hagen A. Simulation of a SOFC/Battery powered vehicle. Int J Hydrog Energy 2019;44(3):1905–18. http://dx.doi.org/10.1016/J.IJHYDENE.2018.11.126.

[34] Zahedi B, Norum LE, Ludvigsen KB. Optimized efficiency of all-electric ships by dc hybrid power systems. J Power Sources 2014;255:341–54. http://dx.doi.org/10.1016/J.JPOWSOUR.2014.01.031.

[35] van Veldhuizen B, Diethelm S, Sahnen D, Thomas A, van Biert L, Visser K. Upscaling and design of an SOFC system for marine applications. In: International marine conference. 2023, URL https://www.researchgate.net/publication/375605556.

[36] Veldhuizen BV, Biert LV, Visser K, Hopman H. Comparative analysis of alternative fuels for marine SOFC systems. In: PRADS. 2022, p. 1240–58.

[37] Salas Ventura S, Metten M, Fortunati D, Ünlübayir C, Diethelm S, Heddrich M, et al. SOFC & Battery hybrid experimental proof of concept and transient simulation for maritime load following. In: 16th EUROPEAN SOFC & SOE FORUM. Lucerne; 2024.

[38] van Veldhuizen B, van Biert L, Amladi A, Woudstra T, Visser K, Aravind P. The effects of fuel type and cathode off-gas recirculation on combined heat and power generation of marine SOFC systems. Energy Convers Manage 2023;276:116498. http://dx.doi.org/10.1016/J.ENCONMAN.2022.116498.

[39] Lai H, Harun NF, Tucker D, Adams TA. Design and eco-technoeconomic analyses of SOFC/GT hybrid systems accounting for long-term degradation effects. Int J Hydrog Energy 2021;46(7):5612–29. http://dx.doi.org/10.1016/J.IJHYDENE.2020.11.032.

[40] Hagen A, Barfod R, Hendriksen PV, Liu Y-L, Ramousse S. Degradation of anode supported SOFCs as a function of temperature and current load. J Electrochem Soc 2006;153(6):A1165. http://dx.doi.org/10.1149/1.2193400.

[41] Abreu-Sepulveda MA, Harun NF, Hackett G, Hagen A, Tucker D. Accelerated degradation for hardware in the loop simulation of fuel cell-gas turbine hybrid system. J Fuel Cell Sci Technol 2015;12(2). http://dx.doi.org/10.1115/1.4028953/371811.

[42] Sheykhi M, Chahartaghi M, Balakheli MM, Hashemian SM, Miri SM, Rafiee N. Performance investigation of a combined heat and power system with internal and external combustion engines. Energy Convers Manage 2019;185:291–303. http://dx.doi.org/10.1016/J.ENCONMAN.2019.01.116.

[43] Ali H, Beltran H, Lindsey NJ, Pecht M. Assessment of the calendar aging of lithium-ion batteries for a long-term—Space missions. Front Energy Res 2023;11. http://dx.doi.org/10.3389/fenrg.2023.1108269.

[44] Preger Y, Barkholtz HM, Fresquez A, Campbell DL, Juba BW, Romàn-Kustas J, et al. Degradation of commercial lithium-ion cells as a function of chemistry and cycling conditions. J Electrochem Soc 2020;167(12):120532. http://dx.doi.org/10.1149/1945-7111/abae37.

[45] Deshpande RD, Uddin K. Physics inspired model for estimating 'cycles to failure' as a function of depth of discharge for lithium ion batteries. J Energy Storage 2021;33. http://dx.doi.org/10.1016/j.est.2020.101932.

[46] Ünlübayir C, Youssfi H, Ahmad R, Salas S, Lilith K, Fortunati D, et al. Comparative analysis and test bench validation of energy management methods for a hybrid marine propulsion system powered by batteries and solid oxide fuel cells. Appl Energy 2024;376(August):124183. http://dx.doi.org/10.1016/j.apenergy.2024.124183.

[47] MG Energy Systems. HE series. 2024, URL https://www.mgenergysystems.eu/en/products/he-series/.

[48] Shin JS, Saqib M, Jo M, Park K, Park KM, Ahn JS, et al. Degradation mechanisms of solid oxide fuel cells under various thermal cycling conditions. ACS Appl Mater Interfaces 2021;13(42):49868–78. http://dx.doi.org/10.1021/acsami.1c13779.